Tarrant, Daniel J., Stirpe, Mariarita, Rowe, Michelle, Howard, Mark J., von der Haar, Tobias and Gourlay, Campbell W. (2016) *Inappropriate expression of the translation elongation factor 1A disrupts genome stability and metabolism.* Journal of Cell Science, 129 . pp. 4455-4465. ISSN 0021-9533.

Inappropriate expression of the translation elongation factor 1A disrupts genome stability and metabolism

Daniel J. Tarrant[1], Mariarita Stirpe[2], Michelle Rowe[1], Mark J. Howard[1], Tobias von der Haar[1]* and Campbell W. Gourlay[1]*

[1]Kent Fungal Group, School of Biosciences, University of Kent, Canterbury, Kent, CT2 7NJ, UK

[2]Deptartment of Biology and Biotechnology, Sapienza, University of Rome.

*authors for correspondence (tv@kent.ac.uk and C.W.Gourlay@kent.ac.uk)

Abstract

The translation elongation factor eEF1A is one of the most abundant proteins found within cells and its role within protein synthesis is well documented. Levels of eEF1A are tightly controlled, with inappropriate expression linked to oncogenesis. However the mechanisms by which increased eEF1A expression alter cell behaviour are unknown. Our analyses in yeast suggest that elevation of eEF1A levels lead to stabilisation of the spindle pole body and changes in nuclear organisation. Elevation of eEF1A2 also leads to altered nuclear morphology in cultured human cells suggesting a conserved role in maintaining genome stability. Gene expression and metabolomic analyses reveal that the level of eEF1A is crucial for the maintenance of metabolism and amino acid levels in yeast, most likely via its role in the control of vacuole function. Increased eEF1A2 levels trigger lysosome biogenesis in cultured human cells, also suggesting a conserved role within metabolic control mechanisms. Together our data suggest that the control of eEF1A levels is important for the maintenance of a number of cell functions out-with translation, whose de-regulation may contribute to its oncogenic properties.

Introduction

The eukaryotic translation elongation factor 1A (eEF1A) is one of the most abundant proteins in the cell, accounting for between 3 and 10% of all soluble protein (Merrick, 1992). It is an essential translation elongation factor which, when bound to GTP delivers aminoacylated-tRNA to the A site of the ribosome. The interaction between mRNA and cognate tRNA within the A site of the ribosome activates eEF1A's GTPase activity leading to the release of its aminoacyl tRNA to the A site of the ribosome. eEF1A·GDP is then released to be recycled to its GTP bound state, allowing it to participate in further rounds of elongation. Alongside this canonical role in translation eEF1A has been reported to be involved in a number of other important cellular functions including actin bundling, nuclear export, apoptosis and the induction of tumour growth (Grosshans et al., 2000; Munshi et al., 2001; Thornton et al., 2003). However despite its importance, the mechanisms by which eEF1A participates in roles out-with translation remain largely uncharacterised.

The yeast *Saccharomyces cerevisiae* possesses two identical eEF1A encoding genes *TEF1* and *TEF2* (Schirmaier and Philippsen, 1984). In contrast eEF1A exists as two variant, tissue specific, isoforms, eEF1A1 and eEF1A2, in all vertebrates. The first, eEF1A1 is expressed in all tissues during development but is no longer detectable in the muscles and heart tissue of adults (Lee et al., 1992; Chambers et al., 1998). Instead high level expression of eEF1A2 is switched on in these tissues, as well as in motor neurons of the medulla (Newbery et al., 2007). The loss of eEF1A2 in mice results in the mutant "wasted mouse" phenotype with symptoms including weight loss, tremors, progressive atrophy of the spleen and thymus leading to death (Chambers et al., 1998). There is also strong evidence implicating eEF1A2 as

a *bona fide* oncogene (Anand et al., 2002). Its levels are elevated in a number of cancer types including breast, ovarian and lung and are correlated to disease progression, decreased lifespan and a poor prognosis (Li et al., 2006; Pinke et al., 2008; Kallioniemi et al., 1994; Anand et al., 2002; Lam et al., 2006). The overexpression of eEF1A2 in Swiss NIH3T3 cells results in enhanced growth rate, anchorage-independent growth, and induced tumour formation when xenografted in nude mice (Anand et al., 2002). Ablation of eEF1A2 in lung cancer models, using short-interfering RNA reduces cell proliferation and promotes apoptosis (Pinke et al., 2008). Given these observations it is likely that eEF1A isoforms participate in a number of as yet uncharacterised cell processes that link cell growth with the process of protein translation.

One example of this is the role that eEF1A is known to play in the control of cytoskeletal stability. eEF1A has a conserved role as an actin-binding protein and this activity has been observed in the yeasts *S. cerevisiae* and *S. pombe*, the slime mould *Dictyostelium discoideum* and in mammalian cell systems (Yang et al., 1990; Edmonds et al., 1996; Suda et al., 1999; Gross and Kinzy, 2005). eEF1A not only binds, but can also cross link F-actin, and in doing so generates actin bundles that possess a unique structure excluding all other actin cross-linkers (Owen et al., 1992). Genetic manipulations of eEF1A have begun to elucidate the mechanism of eEF1A interactions with actin, with residues in domains II and III shown to be important for bundling activity (Gross and Kinzy, 2005; Gross and Kinzy, 2007). Studies have revealed two classes of eEF1A mutations that exhibit separable actin binding and translation elongation functions. The first are those which do not affect the rate of protein synthesis, but result in a disorganised actin cytoskeleton and reduced actin bundling (Gross and Kinzy, 2005). The second class of mutations disrupt actin dynamics, leading to a reduction in

growth rate and a decrease levels of translation initiation (Gross and Kinzy, 2007). The binding sites on eEF1A for aa-tRNA and actin have been shown to overlap (Liu et al., 1996), leading to the suggestion that actin binding and translation activities may be mutually exclusive and that two pools of eEF1A may exist within cells, one actin bound, translation incompetent, and one actively involved in translation. Further to its role in the regulation of the cytoskeleton, eEF1A has the ability to bind to microtubules and influence their stability both *in vitro* and *in vivo* (Shiina et al., 1994; Moore et al., 1998; Tong et al., 2005).

In this study we re-visit the cellular consequences of eEF1A elevation in both yeast and human cells. We find that the elevation of eEF1A levels affects growth and nuclear organisation in both systems. Our data obtained in yeast suggest a new and uncharacterised role for eEF1A in the stability of the spindle pole body and a strong synthetic interaction with the dynactin complex. In addition, our analyses of global gene expression profiles reveal that the elevation of eEF1A levels leads to metabolic changes that are indicative of cell stress. In addition, vacuolar defects associated with increased eEF1A levels are associated with a loss in the regulation of amino acid homeostasis. These effects occur independently of translation, which does not appear to be affected by eEF1A elevation. Our data therefore reveal new insights into the cellular changes that accompany the loss of regulation in eEF1A levels and suggest new mechanisms that may be relevant to the oncogenic properties of this protein.

Materials and Methods

Strains and cell growth

Saccharomyces cerevisiae strains were grown at 30 °C, with liquid cultures grown with rapid aeration at 180 rpm in either YP or synthetic defined media supplemented with 2% glucose. For all experiments cells were grown overnight in selective media and sub-cultured to an OD_{600} of 0.1 before growth analysis. Yeast strains used in this study are described in Table S1. GFP labelled yeast strains were generated as part of a genome wide tagging project (Huh et al., 2003), and obtained from Thermo-Fisher. Growth of yeast in liquid culture was carried out in BMG labtech SPECTROstar Nano plate readers in 24 well or 48 well plates as indicated at a constant temperature of 30°C with orbital shaking at 400rpm and automated OD_{600} determination every 30 min. To generate a eEF1A yeast expression vector a gateway cloning LR reaction was carried out using pENTR/TEV/D-TOPO TEF1 (Havard Medical School PlasmID repository (clone ID ScCD00011628) and pAG425GPD-ccdB. Plasmids expressing Ura3-eEF1A and Ura3-eEF1AK^{333A} were a kind gift from Dr. Stephane Gross (Aston University, UK). To create the eEF1A2 FlipIn HEK293 strain a pcDNA3.0 overexpression plasmid containing eEF1A2 (a kind gift from Jonathan Lee, University of Ottawa, Canada) was digested with HindIII and XhoI and the resultant eEF1A2 ligated into pcDNA5/FRT (Invitrogen). Stable HEK293 cell lines were generated using the Invitrogen Flp-In Recombination System, as per the manufacturers' guidelines. HEK293 cells were grown in a static incubator at 37°C and 5% CO_2 in DMEM, High Glucose, GlutaMAX (Invitrogen, 6195-026) with 2mM glutamine (Invitrogen, 21765-029), 10% FBS (Invitrogen 16000-044) and hygromycin (100µg/ml) in T75 flasks. HEK293 cells were diluted to $5x10^4$/ml and 100 µL applied to the wells of an Xcelligence E-plate for assessment of growth in an RTCA DP analyser (ACEA Bioscience Inc.).

Polysome profiles

For the generation of polysome profiles, cycloheximide was added at a final concentration of 0.1 mg/ml to logarithmically growing yeast cultures (OD_{600} 0.8-09) for five minutes prior to harvest. 60 OD_{600} units of cells were harvested by centrifugation and washed in ice-cold lysis buffer (25 mM Tris-HCl pH 7.5, 100 mM NaCl, 5 mM $MgCl_2$, 5 mM β-mercaptoethanol, 0.1 mg/ml cycloheximide, 0.5 mM PMSF). Washed cells were re-suspended in 700 µl of ice-cold lysis buffer and lysed by six 60 second cycles of vortexing with a volume of acid washed glass beads, with 60 second incubations on ice between cycles. Lysates were cleared by centrifugation at 13000 x g and 450 µl of the cleared lysate were layered onto gradients of 15%-45% sucrose in lysis buffer without PMSF. Gradients were spun for 3 hours at 35,000 rpm and 4°C, and then analysed by passaging through the OD cell of a Bandel BR-188 Gradient Fractionator (Alpha Biotech, UK).

Whole cell protein and metabolite extraction

Whole cell protein extraction was performed from 1×10^8 cells as described (von der Haar, 2007). For detection of metabolites using NMR 50 ml yeast cultures were grown to an OD_{600} of 0.5 and a cell count was performed for quantification purposes. Cells were cooled on ice and washed twice in 25 ml of ice cold water and the wet biomass weighed for quantification purposes. 5ml of boiling 75 % EtOH was added to the pellet together with 2 ml of 0.3 mm glass beads. The samples were vortexed for 30 seconds and then incubated at 80 °C for 3 minutes followed by another 30 second vortex. Samples were decanted into a fresh tube and the beads washed with a further 2 ml of 75 % EtOH that was then combined with the original sample. Samples were then centrifuged at 16,000 g for 10 minutes to remove cell

debris and dried in a Rotorvac at 37 °C. Samples were re-suspended in 330 μl of H_2O and spun at 5000 rpm for 10 minutes to remove any further debris and frozen at -20 °C before being freeze dried.

Metabolite detection by NMR

Experiments were performed at 298 K on a Bruker AVANCE 3 600 MHz spectrometer, equipped with a QCI-F cryoprobe. Data sets were acquired with 64k points and a proton window size of 16 ppm. Spectra were referenced against an internal standard of DSS. Excitation sculpting was used to suppress the water peak using pulsed field gradients. Analysis of data was performed using Bruker TopSpin and AMIX data analysis software. Identification of metabolites was performed by comparison to previously published data on the Madison Metabolomics Consortium Database and by reference to internal standards. We utilised Bruker TopSpin to quantify peak intensity with reference to a DSS standard of known concentration. Absolute concentrations were calculated using Concentration (μM) = peak X intensity/((DSS peak intensity/9 protons)*peak X protons)*50

Assessment of glycogen levels

Strains were grown overnight in SC-LEU medium and re-inoculated to an OD_{600} of 0.1 in fresh SC-LEU medium. Cultures were then grown to an OD_{600} of 0.5 before assessment. $1x10^8$ cells were washed three times in an equivalent volume of de-ionised water followed by three times in ice-cold lysis buffer (25mM sodium citrate, 2.5 mg/ml NaF, pH 4.2) and re-suspended in 100 μl lysis buffer. An equivalent volume of acid washed glass beads were added and cells lysed using a vortex bead beater for three 2 min cycles before being heated to 90°C for 2 min and returned to ice. The homogenate was cleared by centrifugation at 14,000 g for 5 min and

the supernatant used to assess glycogen using the EnzyChrom glycogen assay kit (Bioassay Systems) as per manufacturer's instructions.

Fluorescence microscopy

All fluorescence microscopy was performed on an Olympus IX81 inverted research microscope. Images were captured using a Hamamatsu photonics ORCA AG cooled CCD digital camera, with light excitation from an Olympus MT20 illumination system. Control of the system was through the Olympus CellR imaging software. Images were processed using Huygens deconvolution software from Scientific Volume Imaging.

Immnuofluorescence of yeast cells

Cells were grown to the desired phase of growth and fixed in 5 % formaldehyde for 1 hour. Cells were washed twice in sorbitol buffer (1.2 M sorbitol, 0.1 M potassium phosphate buffer pH7.5), re-suspended in 0.5 ml sorbitol buffer + 1 µl β-mercaptoethanol + 20 µl 1 mg/ml zymolyase and incubated at 37 °C for 40 min. Cells were applied to poly-L-lysine coated welled slides and 10 µl of 0.1 % SDS added for 30 secs before washing ten times with PBS + 1 mg/ml BSA. Immobilised cells were incubated with primary antibody overnight at 4°C. Slides were washed a further ten times with PBS/BSA before adding 15 µl of the secondary anti-body in PBS/BSA at room temperature for 1 hour. Slides were washed ten more times and then a drop of phenylenediamine mounting solution containing DAPI at 1 mg/ml was added before visualisation.

Immunofluorescence of HEK293 cells

HEK293 cells were grown to 70 % confluence on coverslips in six well plates before fixation with 4 % paraformaldehyde in PBS for 15 min. Following fixation cells were permeabilised with 0.1 % TX-100 in PBS for 5 min and then blocked in 250 µl 3 % BSA/PBS for 15 min at room temperature. 25 µl droplets of anti Y-tubulin (1:1000, Sigma GTU88) primary antibody were applied to a sheet of parafilm and the coverslips were placed cell side down on the drops and left in a moist environment overnight at 4°C. Coverslips were then placed on four 100 µl droplets of PBS/0.1 % Tween sequentially and left on each for 5 min to wash. Coverslips were incubated with anti-mouse FITC (1:1000, Sigma) antibody for 1 h at room temperature before being washed a further four times on 100 µl droplets of PBS/ 0.1% Tween and then placed cell side down onto 25 µl droplets of DAPI (1µg/ml) for 1 min followed by two 10 min washes with PBS. 100 µl 0.1 % *p*-Phenylenediamine anti-fade (Sigma P6001-50G) was mixed with 900 µl 10 % mowiol mounting solution (Sigma 81381-50G), 5 µl droplets of this mounting mix were added to glass slides and the coverslips were placed, cell side down, on top of the droplets before visualisation.

ROS detection and PI staining

To assess ROS, cells were grown overnight to stationary phase in the presence of 5 mg/ml 2,7-dichloro dihydrofluorescein diacetate (H2-DCFDA; Molecular Probes). For assessment of PI staining 1×10^7 cells were fixed in 1 ml of ice cold 70% ethanol for 10 min before washing with 1 ml of 50mM Na Citrate. Cells were re-suspended in 0.5ml of 50 mM sodium citrate containing 1mg/ml RNAase A and incubated for 2h at 37^0C before the addition of propidium iodide (PI) to a final concentration of 6 µg/ml. PI staining and ROS levels were assessed using

a BD FACScalibur flow cytometer using FL-2 and FL-1 detection filters respectively. PI stained nuclei were also visualised by fluorescence microscopy using a texas red filter set.

RNA isolation and Microarray

Total RNA was prepared from log phase cells from biological triplicate cultures using a Qiagen RNAeasy kit including an on-column DNAse digestion step according to the manufacturer's instructions. Following reverse transcription reactions the cDNA template was hybridised to an Affymetrix Yeast 2.0 GeneChip array. Data was quality controlled and normalised using the Bioconductor plugin, affylmgui (Wettenhall et al., 2006). To reduce background noise we used the Robust Multi-Array Average (RMA) algorithm (Bolstad et al., 2003). A cut off point was established for genes that were designated to have a B-statistic greater than 1.5. We then sorted the significant data into groups for processing using Gene Ontology (GO) Slim Mapper.

Results

Increased eEF1A levels disrupt nuclear organisation and promote senescence

Given the increasing number of roles assigned to eEF1A out-with translation we sought to further characterise the effects of its overexpression. To achieve this we introduced additional copies of the eEF1A encoding gene, *TEF1*, on a plasmid into wild type yeast cells. Our construct led to a reproducible and stable increase in eEF1A protein level of approximately 80% (Figure 1A). This is a relatively small increase given that the 2μ plasmid employed for overexpression has a typical copy number of 50-100 copies per cell. qPCR assays showed that plasmids containing the *TEF1* gene had a strongly reduced copy number compared to the empty control plasmid (data not shown), consistent with strong selective pressure against overexpression of this gene (Moriya et al., 2006). As expected, the overexpression of eEF1A resulted in fewer, slower growing colonies when compared to control cells (Figure 1B). In liquid growth eEF1A overexpression led to both a reduction in growth rate and an increase in the lag phase prior to growth (Supplementary data Figures S1A and S1B). In agreement with published data ribosomal profiles of actively growing cells overexpressing eEF1A were indistinguishable from controls suggesting that reduced growth was not a result of gross changes in the process of translation (Supplementary data, Figure S2). Interestingly eEF1A overexpression led to a significant reduction in viability as cells entered the stationary phase of growth (Figure 1C). This loss of viability was accompanied by an increase in respiration (Figure 1D) and a lack of cell death markers, such as the accumulation of ROS (Figure 1E). This suggests that increased levels of eEF1A promotes a senescent state as cells experience nutritional depletion.

eEF1A influences dynactin complex stability and spindle assembly

eEF1A is known to interact with the cytoskeleton and has a well-defined ability to bind and bundle actin filaments (Gross and Kinzy, 2005; Owen et al.; Yang et al., 1990). To address whether elevated levels of eEF1A exhibit a synthetic interaction with processes linked to actin function we overexpressed it in a panel of yeast strains deleted for non-essential genes associated with actin organisation or actin-related processes (data not shown). Within this screen we observed synthetic interaction with strains lacking components of the dynactin complex, which has an essential dynein-activating activity and facilitates transport of microtubular associated cargo. The dynactin complex contains the actin-related protein1 (Arp1) which forms an octameric polymer that terminates at its "barbed" end with the actin capping protein CapZ (Schafer et al., 1994) with a further actin-related protein Arp11 placed at the opposite end (Eckley et al., 1999). Projecting from the Arp1 rod is the flexible and extendable side arm that is made up of the remaining three subunits, Nip100 (p150glued), Jnm1 (dynamitin), and Ldb18 (p24) (Figure 2A). As an example of this synthetic interaction we show that overexpression of eEF1A does not result in a further reduction in colony size, as is observed in wild type, in cells lacking the dynactin complex components *ARP1* or *CAP1* when compared to controls (Fig 2B). In addition, the deletion of *ARP1* led to a reduction in time taken to initiate growth (lag phase) which was further reduced upon eEF1A overexpression (Figure 2C).

Dynactin is known to participate in chromosome alignment and nuclear positioning and it has been shown that the deletion of dynactin subunits results in aberrant spindle pole body positioning and chromosome segregation (Maruyama et al., 2002; Yeh et al., 2012). We therefore assessed whether eEF1A levels led to changes in DNA content in actively dividing

cells. Our results suggest that the elevation of eEF1A alone does not result in an increase in aneuploidy (Figure 2D and Supplementary data, Table S2). However, it was observed that all peaks in the FACS spectrum shifted significantly upon eEF1A elevation indicating an increase in dye uptake that may indicate altered nuclear organisation (Figure 2D). In contrast deletion of components of the dynactin complex did lead to an increase in aneuploidy with the emergence of a significant 4N peak (Figure 2D and Supplementary data, Table S2). Interestingly the overexpression of eEF1A in cells lacking dynactin complex components led to a significant additional accumulation of aneuploid cells (Figure 2D and Supplementary data, Table S3 and Figure S3). Our data suggest that elevated eEF1A levels have a significant, translation independent effect upon nuclear organisation. This hypothesis was confirmed by our observation that nuclei of eEF1A overexpressing cells are considerably larger than those wild type control cells (Figure 2E). These larger nuclei were observed to take up more propidium iodide stain, providing an explanation for the increase in fluorescence signal observed by FACS in wild type cells overexpressing eEF1A (Figure 2D).

Next we checked whether elevated eEF1A levels were associated with aberrant spindle organisation in dividing cells via immunofluorescence against β-tubulin (Figure 3A). Spindles in wild type yeast cells originated from the spindle pole body and extended from one tip in the mother cell, to the polar opposite tip in the daughter (Figure 3A). eEF1A overexpression alone did not grossly affect spindle formation and dividing cells appeared similar to wild type (Figure 3A). In contrast cells lacking *ARP1* exhibited aberrant spindle organisation, with cells exhibiting multiple β-tubulin cables (Figure 3A). Interestingly eEF1A overexpression in a *Δarp1* mutant background appeared to prevent the formation of multiple spindles (Figure 3A), however this did not lead to a decrease in aneuploidy (Supplementary data, Table S2).

Spindle pole body positioning and organisation was examined by visualising γ tubulin-GFP (Figure 3B). An increase in eEF1A level resulted in the formation of correctly positioned but visibly larger, brighter spindle pole bodies in wild type cells, suggesting stabilisation of γ tubulin structures (Figure 3B). An increase in eEF1A levels also led to a very significant increase in the presence of Arp1 at the spindle pole (Figure 3B). Considering the canonical roles of dynactin in microtubule anchoring at the spindle pole body and regulation of microtubule dynamics (Quintyne and Schroer, 2002) this presumably reflects an increase in overall spindle pole body stability. The sole known function of dynactin in yeast cells is to facilitate the motor activity of dynein (Moore et al., 2008; Muhua et al., 1994; Eshel et al., 1993). In support of the elevation of eEF1A stabilising the spindle pole body we also observed an accumulation of GFP labelled dynein heavy chain, Dhc1 (Figure 3C). The increased spindle pole body stability, shown here by the accumulation of Arp1 at the spindle pole boy (Figure 3D), was not observed upon expression of a mutant isoform of eEF1A, eEF1A[K333E], that is well documented to be unable to bind to actin (Figure 3D). Taken together these data suggest that an excess of eEF1A leads to the stabilisation of the spindle pole body via its interaction with actin in yeast cells which in turn affects genome integrity.

Elevated levels of human eEF1A2 affect growth and nuclear organisation in HEK293 cells

Elevated levels of eEF1A2 have been found in many tumours, and expression of eEF1A2 in non-native tissues is known to induce tumourigenesis (Anand et al., 2002). Given our findings in the yeast system we generated eEF1A2 expressing human embryonic kidney 293 (HEK293) cells (Figure 4A) to examine whether its elevation also affected the control of cell growth control and nuclear organisation. HEK293 cells were selected as they do not express eEF1A2 and so serve to highlight the effects of inappropriate expression of this isoform.

Initially we assessed the effects of eEF1A2 on growth using an Xcelligence RTCA DP Analyser. This is an automated system that allows analysis of attachment and growth of adherent cell lines by continuous measurement of the impedance of an electric current across a gold plated well. Cell growth is measured as an increase in impedance and reported as a Cell Index (CI) value. This analysis revealed that, as has been reported to occur in NIH3T3 cells (Anand et al., 2002), an increase in eEF1A2 leads to a reproducible reduction in doubling time in HEK293 cells (Figure 4B). HEK293 cells overexpressing eEF1A2 also initiated surface attachment more rapidly than controls (Figure 4C) and appeared to spread less on the surface of tissue culture vessels leading to both a rounded appearance and displayed a disorganised microtubular cytoskeleton (Data not shown). FACS analysis and microscopy revealed that, as had been observed in yeast, the expression of eEF1A2 did not lead to an increase in aneuploidy but did result in a significant shift in the fluorescent signal from 2C and 4C peaks (Figure 4D). This finding was consistent with our observation that, as had been observed in yeast, eEF1A2 cells possessed enlarged nuclei (Figure 4E). However, in contrast to our findings in the yeast system we did not observe differences in gamma-tubulin distribution at the centrosome within the mitotic HEK293 control of eEF1A2 expressing cells (Figure 4F). These results suggest that the elevation of eEF1A affects both growth and nuclear architecture in HEK293 cells.

Increased eEF1A levels modify carbon flux within yeast cells

Given our observations that elevated levels of eEF1A lead to genomic instability in yeast we sought to determine its effects upon gene expression during log phase growth using a microarray approach. Upon overexpression of eEF1A we found that a total of 319 genes were up- and 61 down-regulated during log phase when a B-statistic of 1.5 was applied as a

cut off threshold (Supplementary data Tables S3 and S4). A number of indicators of cell stress were present within the data set including the upregulation of genes involved in response to osmotic stress, starvation, cell wall stress and heat shock (Supplementary data Table S3). The most highly enriched biological processes were those of carbohydrate transport and processing (Supplementary data Table S3). Upon closer analysis we found that genes involved in glucose uptake (*HXT1, HXT6, HXT7* and *HXT9*) and all steps required for its processing into the stress linked and storage di- and poly-saccharides trehalose and glycogen were upregulated (Figure 5A). We verified that cells overexpressing eEF1A accumulated trehalose during log phase growth using a quantitative NMR approach (Figure 5B and 5C). A three-fold increase in trehalose levels in cells expressing eEF1A was observed when compared to controls (Figure 5B and 5C). As a unique NMR peak could not be determined for glycogen we analysed its levels during log phase growth using a biochemical assay (Figure 5D). Surprisingly despite an upregulation in glycogen biosynthesis genes we observed that glycogen levels appeared lower than wild type when eEF1A was overexpressed (Figure 5D). This may be a result of the upregulation of the glycogen debranching and mobilisation enzymes Gdb1 and Gph1 respectively in cells overexpressing eEF1A (Fig 5A and Supplementary data Table S3). As we had observed a synthetic interaction between increased eEF1A levels and dynactin complex integrity we also checked whether the deletion of *ARP1* induced glycogen accumulation (Figure 5D). We observed that cells lacking ARP1 also had reduced glycogen levels when compared to wild type that were slightly raised when eEF1A was overexpressed (Figure 5D). Together these data suggest that the elevation of eEF1A in yeast leads to a significant alteration in the flow of carbon during growth towards the accumulation of the stress linked disaccharide trehalose.

Increased eEF1A levels disrupt amino acid homeostasis and vacuole function

Our microarray analysis revealed an increase in a number of genes involved in the regulation of amino acid transport and metabolism (Supplementary data, Table S3). We hypothesised that elevated levels of eEF1A may therefore impact upon the regulation of amino acid levels. To investigate this further we employed an NMR metabolomics approach. We produced metabolite extracts from six independent actively growing yeast cultures to determine the effects of eEF1A overexpression (Figure 6A, Table 1 and Supplementary data, Figure S4). From the NMR spectrum we were able to determine that the levels of a number of amino acids including isoleucine, leucine, alanine, valine, glutamate and lysine were significantly elevated upon eEF1A overexpression (Figure 6A and Table 1). The presence of amino acid stress in cells overexpressing eEF1A is further supported within our gene expression data as we observed the upregulation of several transporters, such as the aspartate transporter, *AVT6*, and the high affinity branched amino acid permease, *BAP2* (Supplementary data, Table S3). Further evidence that changes in metabolic homeostasis occur upon eEF1A overexpression as both NADH and acetic acid levels were significantly reduced (Table 1). The vacuole is the major amino acid storage and distribution organelle in yeast cells and it serves a similar purpose with respect to carbohydrates such as trehalose (Jules et al., 2004; Wilson et al., 2002). As the actin cytoskeleton plays an important role in controlling vacuole biogenesis and function (Bodman et al., 2015) and given the known role for eEF1A in controlling actin dynamics we hypothesised that the function of this organelle may be impaired upon its overexpression. To investigate this we made use of fluorescent dyes, MDY-64, CMAC and Quinacrine that stain the membrane or accumulate in the lumen of functional and acidified vacuoles. In all cases the overexpression of eEF1A led to a failure to incorporate each dye to the extent observed in wild type cells indicating vacuole

dysfunction (Figure 6B). Interestingly a significant increase in lysosome biogenesis was also observed in HEK293 cells overexpressing eEF1A2 (Figure 6C). As lysosomes are the functional equivalent of the yeast vacuole this finding suggests a conserved role for eEF1A in the control of metabolism. Together these data suggest that eEF1A overexpression may perturb metabolic homeostasis through interactions with the vacuolar compartment in yeast and lysosomes in human cells.

Discussion

Although its canonical role in translation elongation is well characterised, the moonlighting functions of eEF1A and the effects of loss of its regulation poorly understood. The importance of maintaining the control of eEF1A levels is highlighted by the oncogenic properties of eEF1A2, whose inappropriate expression has been shown to induce tumour growth. To increase our understanding of the consequences of an increase in eEF1A above normal levels we made use of the highly amenable budding yeast *S. cerevisiae*. Previous studies on eEF1A overexpression in yeast revealed links to altered actin cytoskeletal organisation that correlated with changes in growth (Munshi et al., 2001). These effects were attributed to the ability of eEF1A to bind to and bundle actin fibres (Gross and Kinzy, 2005), although the mechanisms that underlie its effects on growth were not identified. Here we report that the elevation of eEF1A promotes genome instability and metabolic changes in both yeast and human cells that may contribute to its effects upon growth.

In the yeast system we observed a strong synthetic genetic interaction between eEF1A and the dynactin complex. In higher eukaryotic systems dynactin can be found in a variety of subcellular localisations, for example within centrosomes (spindle pole bodies in yeast), and within a variety of endomembranes (Chen et al., 2015; Gill et al., 1991; Paschal et al., 1993; Habermann et al., 2001). Dynactin is implicated in the regulation of dynein targeting and/or recruitment and facilities its processivity along microtubules. At the centrosome, dynactin and dynein are important in microtubule anchoring (Quintyne et al., 1999) and this function is conserved in the yeast system (Muhua et al., 1994). Dynactin is also able to control microtubule dynamics and recruit proteins to the plus ends of microtubules (Quintyne et al.,

1999; Yeh et al., 2012).The localisation of dynactin to the cell cortex allows it to influence rotational movement of the mitotic spindle and direct movement of motile cells (Skop and White, 1998; Gönczy et al., 1999; Dujardin et al., 2003). However despite the plethora of known roles in higher eukaryotes the only known function of dynactin in yeast cells is in the control of spindle pole body dynamics (Moore et al., 2008). Our data suggests that eEF1A may influence genome stability via spindle pole body stabilisation and that this activity is revealed upon combination with additional defects in spindle pole body organisation. In line with this hypothesis an increase in eEF1A levels dramatically increased the aneuploidy observed in yeast cells lacking core dynactin complex components. In addition, eEF1A overexpression in yeast led to the accumulation of γ-tubulin and the dynactin/dynein complex at the spindle pole body. These data indicate that an increase in eEF1A levels leads to stabilisation of the spindle pole body, with downstream effects upon nuclear organisation and genome stability. One possibility is that eEF1A is an unrecognised component of the spindle pole body, perhaps via its known role as a cytoskeletal binding protein. One may envisage that the stabilisation of the spindle pole body upon overexpression of eEF1A may arise from a stabilising effect upon actin or γ-tubulin structures therein. However exhaustive studies on the composition of the spindle pole body in yeast have not identified it as a component part (Kilmartin, 2014; Wigge, 1998). It does remain a possibility that eEF1A may function within the spindle pole body under specific cellular conditions or indeed become incorporated when its levels become elevated.

As well as containing microtubules, the spindle pole body in yeast relies on the functions of the actin cytoskeleton for positioning. Indeed there exists a strict cooperativity between the actin and microtubular cytoskeletons in positioning the spindle pole body to ensure faithful

segregation of chromosomes. It seems likely therefore that an increase in eEF1A level perturbs nuclear stability via its role in regulating the stability of the actin cytoskeleton. In line with this we observed that the expression of a mutant form of eEF1A, eEF1A^{K333A} which cannot bind to actin, did not lead to spindle pole body defects upon overexpression. The expression of eEF1A^{K333A} has also been shown to have no effect upon growth rate in yeast cells (Gross and Kinzy, 2005). Interestingly the overexpression of eEF1A alone did not appear to increase the generation of aneuploid cells, as was the case upon loss of the dynactin complex, and did not affect positioning of the spindle pole body. These data suggest that the effects of eEF1A upon spindle pole body do not occur via the inactivation of dynactin function. A more likely explanation is that an actin dependent stabilisation of the spindle pole body leads to the accumulation of dynactin and dynein with downstream effects upon nuclear organisation. However the levels of γ-tubulin are reported to increase in response to DNA replication stress (Tkach et al., 2012). We cannot therefore rule out the possibility that the effects of eEF1A overexpression on spindle organisation, and chromosomal segregation are also influenced by a stress response that in turn leads to SPB stabilisation. A role for actin in the regulation of chromosome dynamics in yeast has recently been described in which both cytoplasmic and nuclear actin structures were implicated (Spichal et al., 2016). An extension of these findings is that stabilisation of actin structures via eEF1A overexpression may alter the dynamic interplay between chromosomes and the nuclear envelope in addition to stabilisation of the spindle pole body. This relationship may in turn have an effect upon entry into the cell cycle as we observe significant changes in the lag phase of growth when eEF1A is overexpressed. It may be that such a role is conserved as we also noted changes in nuclear morphology in HEK293 cells expressing eEF1A2. In both yeast and HEK293 cells we observed that eEF1A overexpression led to an increase in nuclear size.

This size increase was accompanied by an increase in propidium iodide staining, a phenomena that has been reported to occur upon a reduction in histone occupancy, which in turn reveals more dye binding sites (Giangarè et al., 1989). It will be of interest to fully characterise the nuclear changes that occur as a result of eEF1A overexpression and to determine whether these findings are linked to the oncogenic properties of eEF1A2.

Our analyses demonstrate that increasing eEF1A levels lead to the coordinated upregulation of glucose uptake and its storage within trehalose. This raises the possibility that spindle pole body stabilisation may in turn trigger carbohydrate storage, perhaps via changes in gene expression leading from changes in chromatin. Indeed it has been reported that DNA damage can lead to the activation of storage carbohydrate synthesis in yeast (Kitanovic et al., 2009). However the deletion of *ARP1*, which leads to severe defects in spindle organisation and chromosome segregation, did not lead to the accumulation of glycogen when compared to wild type. Similar results were obtained for other strains lacking dynactin complex components (data not shown) suggesting that another mechanism may be responsible for the changes in metabolic activity observed. Recent data suggests that the *TPS1* gene, which encodes the synthase subunit of trehalose-6-P synthase and which was upregulated in response to eEF1A overexpression, plays an important role in managing diverse stress responses and protection against apoptosis independently of its role in trehalose biosynthesis (Petitjean et al., 2015; Petitjean et al., 2016). This may be important given our finding that eEF1A overexpression does not lead to an increase in cell death despite its effects on nuclear stability, but instead increases metabolic functions within the cell.

Our metabolomic and gene expression profiling data suggest that the elevation of eEF1A levels leads to changes in the levels of a number of amino acids within dividing cells. The vacuole represents an important organelle that is a site for the storage of amino acids and carbohydrates. The processes of uptake and release from the vacuole are active and require the function of membrane localised transporters (Kucharczyk and Rytka, 2001). Our data suggest that the function of the vacuole becomes impaired upon the expression of eEF1A and our preliminary findings suggest that under these conditions vacuoles are found to contain amino acid levels that differ significantly from that of wild type (data not shown). Whether amino acid storage, transport or sensing mechanisms underlie the defects induced by an increase in eEF1A levels requires further investigation. A possible mechanism to explain the loss of control of vacuole function may rest with the ability of eEF1A to stabilise actin filaments. The function of the vacuole has been shown to be linked to actin filament construction, which is important for maintaining organelle stability. In support of this hypothesis it has recently been published that eEF1A and actin interact to control vacuole stability in yeast (Bodman et al., 2015). A model is proposed whereby eEF1A binds to the small GTPase Rho1p on the vacuolar membrane. Upon activation of Rho1, eEF1A is released and acts to stabilise the vacuole via its actin bundling activity (Bodman et al., 2015). One possibility is therefore that elevation of eEF1A leads to vacuolar defects via a similar mechanism resulting in an inability to control amino acid levels. However as we do not observe vacuolar morphological defects, but instead a loss of membrane potential and acidification, it may be the case that eEF1A interacts directly or indirectly with the vATPase to inhibit its function. Interestingly, expression of eEF1A2 in HEK293 cells led to a dramatic accumulation of lysosomes when compared to controls. This result requires further investigation but may suggest the induction of autophagy, which results in lysosome

proliferation, or alternatively the activation of a lysosome biogenesis programme. It is unclear whether an increase in eEF1A levels perturbs vacuole and lysosome functions via a similar mechanism or whether these results reflect more general responses to metabolic disruption. Interestingly, and in line with a role for eEF1A2 as an oncogene, the upregulation of lysosome biogenesis has been reported to be important for the support of cancer cell metabolic requirements (Perera et al., 2015).

Our experiments have identified two new apparently distinct changes in cell behaviour that are associated with an increase in eEF1A levels. The discovery that nuclear organisation and metabolic homeostasis are directly influenced by eEF1A levels may be of importance with respect to its ability to act as an oncogene. These effects may be attributable to the role that eEF1A plays in the stabilisation of cytoskeletal structures. It will be important to further characterise the roles and interactions of eEF1A if we are to fully understand its oncogenic properties.

References

Anand, N., Murthy, S., Amann, G., Wernick, M., Porter, L. A., Cukier, I. H., Collins, C., Gray, J. W., Diebold, J., Demetrick, D. J., et al. (2002). Protein elongation factor EEF1A2 is a putative oncogene in ovarian cancer. *Nat. Genet.* **31**, 301–5.

Bodman, J. A. R., Yang, Y., Logan, M. R. and Eitzen, G. (2015). Yeast translation elongation factor-1A binds vacuole-localized Rho1p to facilitate membrane integrity through F-actin remodeling. *J. Biol. Chem.* **290**, 4705–16.

Bolstad, B. M., Irizarry, R. A., Astrand, M. and Speed, T. P. (2003). A comparison of normalization methods for high density oligonucleotide array data based on variance and bias. *Bioinformatics* **19**, 185–93.

Chambers, D. M., Peters, J. and Abbott, C. M. (1998). The lethal mutation of the mouse wasted (wst) is a deletion that abolishes expression of a tissue-specific isoform of translation elongation factor 1alpha, encoded by the Eef1a2 gene. *Proc. Natl. Acad. Sci. U. S. A.* **95**, 4463–8.

Chen, T.-Y., Syu, J.-S., Han, T.-Y., Cheng, H.-L., Lu, F.-I. and Wang, C.-Y. (2015). Cell Cycle-Dependent Localization of Dynactin Subunit p150(glued) at Centrosome. *J. Cell. Biochem.* **116**, 2049–60.

Dujardin, D. L., Barnhart, L. E., Stehman, S. A., Gomes, E. R., Gundersen, G. G. and Vallee, R. B. (2003). A role for cytoplasmic dynein and LIS1 in directed cell movement. *J. Cell Biol.* **163**, 1205–11.

Eckley, D. M., Gill, S. R., Melkonian, K. A., Bingham, J. B., Goodson, H. V, Heuser, J. E. and Schroer, T. A. (1999). Analysis of dynactin subcomplexes reveals a novel actin-related protein associated with the arp1 minifilament pointed end. *J. Cell Biol.* **147**, 307–20.

Edmonds, B. T., Wyckoff, J., Yeung, Y. G., Wang, Y., Stanley, E. R., Jones, J., Segall, J. and Condeelis, J. (1996). Elongation factor-1 alpha is an overexpressed actin binding protein in metastatic rat mammary adenocarcinoma. *J. Cell Sci.* **109 (Pt 1**, 2705–14.

Eshel, D., Urrestarazu, L. A., Vissers, S., Jauniaux, J. C., van Vliet-Reedijk, J. C., Planta, R. J. and Gibbons, I. R. (1993). Cytoplasmic dynein is required for normal nuclear segregation in yeast. *Proc. Natl. Acad. Sci. U. S. A.* **90**, 11172–6.

Giangarè, M. C., Prosperi, E., Pedrali-Noy, G. and Bottiroli, G. (1989). Flow cytometric evaluation of DNA stainability with propidium iodide after histone H1 extraction. *Cytometry* **10**, 726–30.

Gill, S. R., Schroer, T. A., Szilak, I., Steuer, E. R., Sheetz, M. P. and Cleveland, D. W. (1991). Dynactin, a conserved, ubiquitously expressed component of an activator of vesicle motility mediated by cytoplasmic dynein. *J. Cell Biol.* **115**, 1639–50.

Gönczy, P., Pichler, S., Kirkham, M. and Hyman, A. A. (1999). Cytoplasmic dynein is required for distinct aspects of MTOC positioning, including centrosome separation, in the one cell stage Caenorhabditis elegans embryo. *J. Cell Biol.* **147**, 135–50.

Gross, S. R. and Kinzy, T. G. (2005). Translation elongation factor 1A is essential for regulation of the actin cytoskeleton and cell morphology. *Nat. Struct. Mol. Biol.* **12**, 772–8.

Gross, S. R. and Kinzy, T. G. (2007). Improper organization of the actin cytoskeleton affects protein synthesis at initiation. *Mol. Cell. Biol.* **27**, 1974–89.

Grosshans, H., Hurt, E. and Simos, G. (2000). An aminoacylation-dependent nuclear tRNA export pathway in yeast. *Genes Dev.* **14**, 830–40.

Habermann, A., Schroer, T. A., Griffiths, G. and Burkhardt, J. K. (2001). Immunolocalization of cytoplasmic dynein and dynactin subunits in cultured macrophages: enrichment on early endocytic organelles. *J. Cell Sci.* **114**, 229–240.

Huh, W.-K., Falvo, J. V, Gerke, L. C., Carroll, A. S., Howson, R. W., Weissman, J. S. and O'Shea, E. K. (2003). Global analysis of protein localization in budding yeast. *Nature* **425**, 686–91.

Jules, M., Guillou, V., François, J. and Parrou, J.-L. (2004). Two distinct pathways for trehalose assimilation in the yeast Saccharomyces cerevisiae. *Appl. Environ. Microbiol.* **70**, 2771–8.

Kallioniemi, A., Kallioniemi, O. P., Piper, J., Tanner, M., Stokke, T., Chen, L., Smith, H. S., Pinkel, D., Gray, J. W. and Waldman, F. M. (1994). Detection and mapping of amplified DNA sequences in breast cancer by comparative genomic hybridization. *Proc. Natl. Acad. Sci. U. S. A.* **91**, 2156–60.

Kilmartin, J. V (2014). Lessons from yeast: the spindle pole body and the centrosome. *Philos. Trans. R. Soc. Lond. B. Biol. Sci.* **369**,.

Kitanovic, A., Walther, T., Loret, M. O., Holzwarth, J., Kitanovic, I., Bonowski, F., Van Bui, N., Francois, J. M. and Wölfl, S. (2009). Metabolic response to MMS-mediated DNA damage in Saccharomyces cerevisiae is dependent on the glucose concentration in the medium. *FEMS Yeast Res.* **9**, 535–51.

Kucharczyk, R. and Rytka, J. (2001). Saccharomyces cerevisiae--a model organism for the studies on vacuolar transport. *Acta Biochim. Pol.* **48**, 1025–42.

Lam, D. C. L., Girard, L., Suen, W.-S., Chung, L., Tin, V. P. C., Lam, W., Minna, J. D. and Wong, M. P. (2006). Establishment and expression profiling of new lung cancer cell lines from Chinese smokers and lifetime never-smokers. *J. Thorac. Oncol.* **1**, 932–42.

Lee, S., Francoeur, A. M., Liu, S. and Wang, E. (1992). Tissue-specific expression in mammalian brain, heart, and muscle of S1, a member of the elongation factor-1 alpha gene family. *J. Biol. Chem.* **267**, 24064–8.

Li, R., Wang, H., Bekele, B. N., Yin, Z., Caraway, N. P., Katz, R. L., Stass, S. A. and Jiang, F. (2006). Identification of putative oncogenes in lung adenocarcinoma by a comprehensive functional genomic approach. *Oncogene* **25**, 2628–35.

Liu, G., Tang, J., Edmonds, B. T., Murray, J., Levin, S. and Condeelis, J. (1996). F-actin

sequesters elongation factor 1alpha from interaction with aminoacyl-tRNA in a pH-dependent reaction. *J. Cell Biol.* **135**, 953–63.

Maruyama, J., Nakajima, H. and Kitamoto, K. (2002). Observation of EGFP-visualized nuclei and distribution of vacuoles in Aspergillus oryzae arpA null mutant. *FEMS Microbiol. Lett.* **206**, 57–61.

Merrick, W. C. (1992). Mechanism and regulation of eukaryotic protein synthesis. *Microbiol. Rev.* **56**, 291–315.

Moore, R. C., Durso, N. A. and Cyr, R. J. (1998). Elongation factor-1alpha stabilizes microtubules in a calcium/calmodulin-dependent manner. *Cell Motil. Cytoskeleton* **41**, 168–80.

Moore, J. K., Li, J. and Cooper, J. A. (2008). Dynactin function in mitotic spindle positioning. *Traffic* **9**, 510–27.

Moriya, H., Shimizu-Yoshida, Y. and Kitano, H. (2006). In vivo robustness analysis of cell division cycle genes in Saccharomyces cerevisiae. *PLoS Genet.* **2**, e111.

Muhua, L., Karpova, T. S. and Cooper, J. A. (1994). A yeast actin-related protein homologous to that in vertebrate dynactin complex is important for spindle orientation and nuclear migration. *Cell* **78**, 669–79.

Munshi, R., Kandl, K. A., Carr-Schmid, A., Whitacre, J. L., Adams, A. E. and Kinzy, T. G. (2001). Overexpression of translation elongation factor 1A affects the organization and function of the actin cytoskeleton in yeast. *Genetics* **157**, 1425–36.

Newbery, H. J., Loh, D. H., O'Donoghue, J. E., Tomlinson, V. A. L., Chau, Y.-Y., Boyd, J. A., Bergmann, J. H., Brownstein, D. and Abbott, C. M. (2007). Translation elongation factor eEF1A2 is essential for post-weaning survival in mice. *J. Biol. Chem.* **282**, 28951–9.

Owen, C. H., DeRosier, D. J. and Condeelis, J. (1992) Actin crosslinking protein EF-1a of Dictyostelium discoideum has a unique bonding rule that allows square-packed bundles. *J. Struct. Biol.* **109**, 248–54.

Paschal, B. M., Holzbaur, E. L., Pfister, K. K., Clark, S., Meyer, D. I. and Vallee, R. B. (1993). Characterization of a 50-kDa polypeptide in cytoplasmic dynein preparations reveals a complex with p150GLUED and a novel actin. *J. Biol. Chem.* **268**, 15318–23.

Perera, R. M., Stoykova, S., Nicolay, B. N., Ross, K. N., Fitamant, J., Boukhali, M., Lengrand, J., Deshpande, V., Selig, M. K., Ferrone, C. R., et al. (2015). Transcriptional control of autophagy-lysosome function drives pancreatic cancer metabolism. *Nature* **524**, 361–5.

Petitjean, M., Teste, M.-A., François, J. M. and Parrou, J.-L. (2015). Yeast Tolerance to Various Stresses Relies on the Trehalose-6P Synthase (Tps1) Protein, Not on Trehalose. *J. Biol. Chem.* **290**, 16177–90.

Petitjean, M., Teste, M.-A., Léger-Silvestre, I., François, J. M. and Parrou, J.-L. (2016). A new function for the yeast trehalose-6P synthase (Tps1) protein, as key pro-survival

factor during growth, chronological ageing, and apoptotic stress. *Mech. Ageing Dev.*

Pinke, D. E., Kalloger, S. E., Francetic, T., Huntsman, D. G. and Lee, J. M. (2008). The prognostic significance of elongation factor eEF1A2 in ovarian cancer. *Gynecol. Oncol.* **108**, 561–8.

Quintyne, N. J. and Schroer, T. A. (2002). Distinct cell cycle-dependent roles for dynactin and dynein at centrosomes. *J. Cell Biol.* **159**, 245–54.

Quintyne, N. J., Gill, S. R., Eckley, D. M., Crego, C. L., Compton, D. A. and Schroer, T. A. (1999). Dynactin is required for microtubule anchoring at centrosomes. *J. Cell Biol.* **147**, 321–34.

Schafer, D. A., Gill, S. R., Cooper, J. A., Heuser, J. E. and Schroer, T. A. (1994). Ultrastructural analysis of the dynactin complex: an actin-related protein is a component of a filament that resembles F-actin. *J. Cell Biol.* **126**, 403–12.

Schirmaier, F. and Philippsen, P. (1984). Identification of two genes coding for the translation elongation factor EF-1 alpha of S. cerevisiae. *EMBO J.* **3**, 3311–5.

Shiina, N., Gotoh, Y., Kubomura, N., Iwamatsu, A. and Nishida, E. (1994). Microtubule severing by elongation factor 1 alpha. *Science* **266**, 282–5.

Skop, A. R. and White, J. G. (1998). The dynactin complex is required for cleavage plane specification in early Caenorhabditis elegans embryos. *Curr. Biol.* **8**, 1110–6.

Spichal, M., Brion, A., Herbert, S., Cournac, A., Marbouty, M., Zimmer, C., Koszul, R. and Fabre, E. (2016). Evidence for a dual role of actin in regulating chromosome organization and dynamics in yeast. *J. Cell Sci.* **129**, 681–92.

Suda, M., Fukui, M., Sogabe, Y., Sato, K., Morimatsu, A., Arai, R., Motegi, F., Miyakawa, T., Mabuchi, I. and Hirata, D. (1999). Overproduction of elongation factor 1alpha, an essential translational component, causes aberrant cell morphology by affecting the control of growth polarity in fission yeast. *Genes Cells* **4**, 517–27.

Teste, M. A., Enjalbert, B., Parrou, J. L. and François, J. M. (2000). The Saccharomyces cerevisiae YPR184w gene encodes the glycogen debranching enzyme. *FEMS Microbiol. Lett.* **193**, 105–10.

Thornton, S., Anand, N., Purcell, D. and Lee, J. (2003). Not just for housekeeping: protein initiation and elongation factors in cell growth and tumorigenesis. *J. Mol. Med. (Berl).* **81**, 536–48.

Tkach, J. M., Yimit, A., Lee, A. Y., Riffle, M., Costanzo, M., Jaschob, D., Hendry, J. A., Ou, J., Moffat, J., Boone, C., et al. (2012). Dissecting DNA damage response pathways by analysing protein localization and abundance changes during DNA replication stress. *Nat. Cell Biol.* **14**, 966–76.

Tong, T., Ji, J., Jin, S., Li, X., Fan, W., Song, Y., Wang, M., Liu, Z., Wu, M. and Zhan, Q. (2005). Gadd45a expression induces Bim dissociation from the cytoskeleton and translocation to mitochondria. *Mol. Cell. Biol.* **25**, 4488–500.

von der Haar, T. (2007). Optimized protein extraction for quantitative proteomics of yeasts. *PLoS One* **2**, e1078.

Wettenhall, J. M., Simpson, K. M., Satterley, K. and Smyth, G. K. (2006). affylmGUI: a graphical user interface for linear modeling of single channel microarray data. *Bioinformatics* **22**, 897–9.

Wigge, P. A. (1998). Analysis of the Saccharomyces Spindle Pole by Matrix-assisted Laser Desorption/Ionization (MALDI) Mass Spectrometry. *J. Cell Biol.* **141**, 967–977.

Wilson, W. A., Wang, Z. and Roach, P. J. (2002). Systematic identification of the genes affecting glycogen storage in the yeast Saccharomyces cerevisiae: implication of the vacuole as a determinant of glycogen level. *Mol. Cell. Proteomics* **1**, 232–42.

Yang, F., Demma, M., Warren, V., Dharmawardhane, S. and Condeelis, J. (1990). Identification of an actin-binding protein from Dictyostelium as elongation factor 1a. *Nature* **347**, 494–6.

Yeh, T.-Y., Quintyne, N. J., Scipioni, B. R., Eckley, D. M. and Schroer, T. A. (2012). Dynactin's pointed-end complex is a cargo-targeting module. *Mol. Biol. Cell* **23**, 3827–37.

Acknowledgments

A

Wild type   + eEF1A

2µl   10µl   2µl   10µl

eEF1A

Sypro Red

B

10^4 10^3 10^2

Wild type
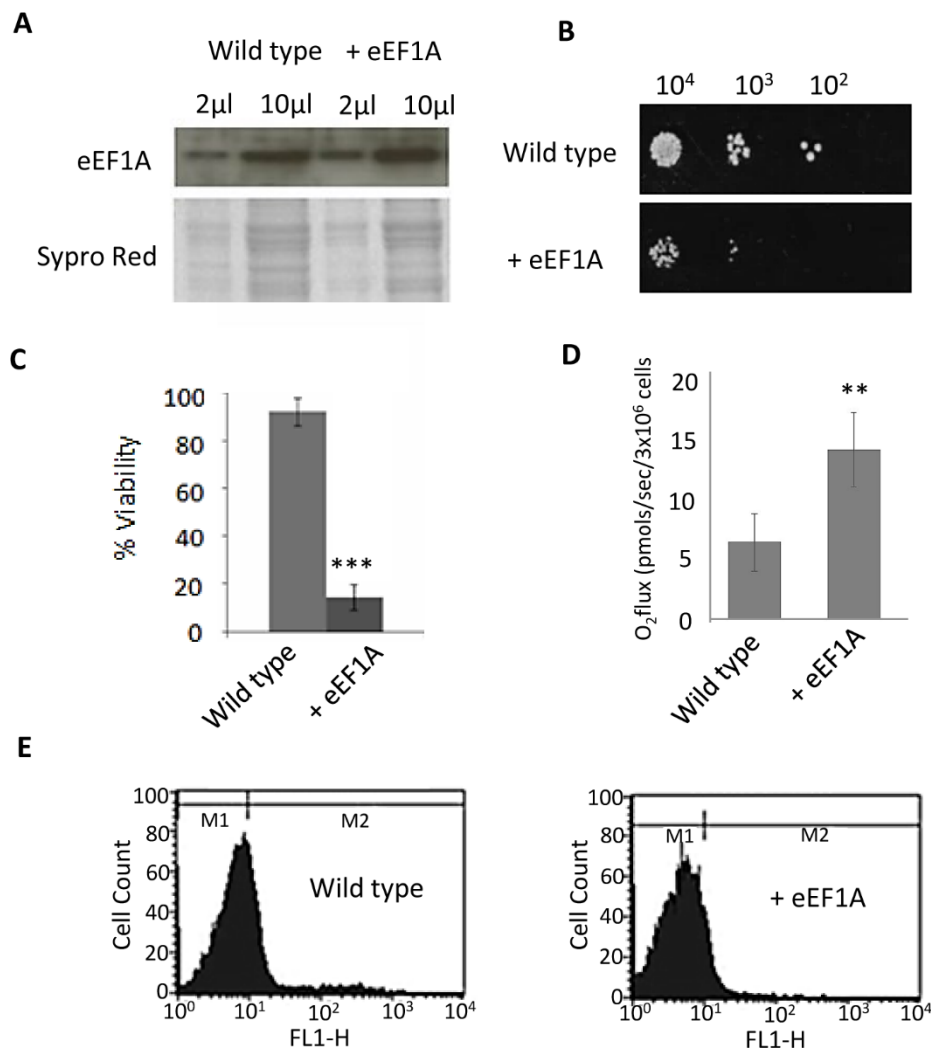
+ eEF1A

C

D

E

Figure 1 – An empty multi-copy control plasmid or one containing eEF1A under the control of a GPD promoter was introduced into a wild type yeast strain and grown on selective media. Levels of eEF1A were assessed by western blot following protein extraction using a quantitative method (von der Haar, 2007). Two different volumes were loaded to help assess changes in eEF1A level that were measured by densitometry using image J and loading differences corrected using sypro red staining (A). The effects of eEF1A overexpression were assayed by spotting a serial dilution series of cells taken from cultures

grown to log phase (B). Viability of cells within a culture grown for 24h to early stationary phase in synthetic media lacking leucine + 2% glucose was assessed by a colony forming unit assay, n = 3 (C). Oxygen consumption was measured using a high resolution respirometer (D) and ROS production was measured by flow cytometry using $H_2DCF-DA$ (E) were also measured after 24h growth to early stationary phase in synthetic media lacking leucine + 2% glucose (n = 3). Error bars represent standard deviation, ***P<0.001, **P<0.01.

Figure 2 – A schematic of the yeast dynactin complex is presented (A). The effects of eEF1A

overexpression upon colony size are shown in Wild type, *Δarp1* and *Δcap1* cells, two

independent transformants are shown (i and ii) (B). The effect of eEF1A overexpression on

time taken to initiate growth following inoculation, or lag phase were calculated in wild type

and *Δarp1* cells (n = 3, standard deviation is presented) (C). DNA content was analysed in

Wild type or *Δarp1* cells containing a control (filled) or eEF1A overexpression (open) plasmid

using flow cytometry following propidium iodide staining (D). Propidium iodide stained

nuclei from wild type or *Δarp1* cells containing a control or eEF1A overexpression plasmid

were visualised using fluorescence microscopy and their size determined using image j

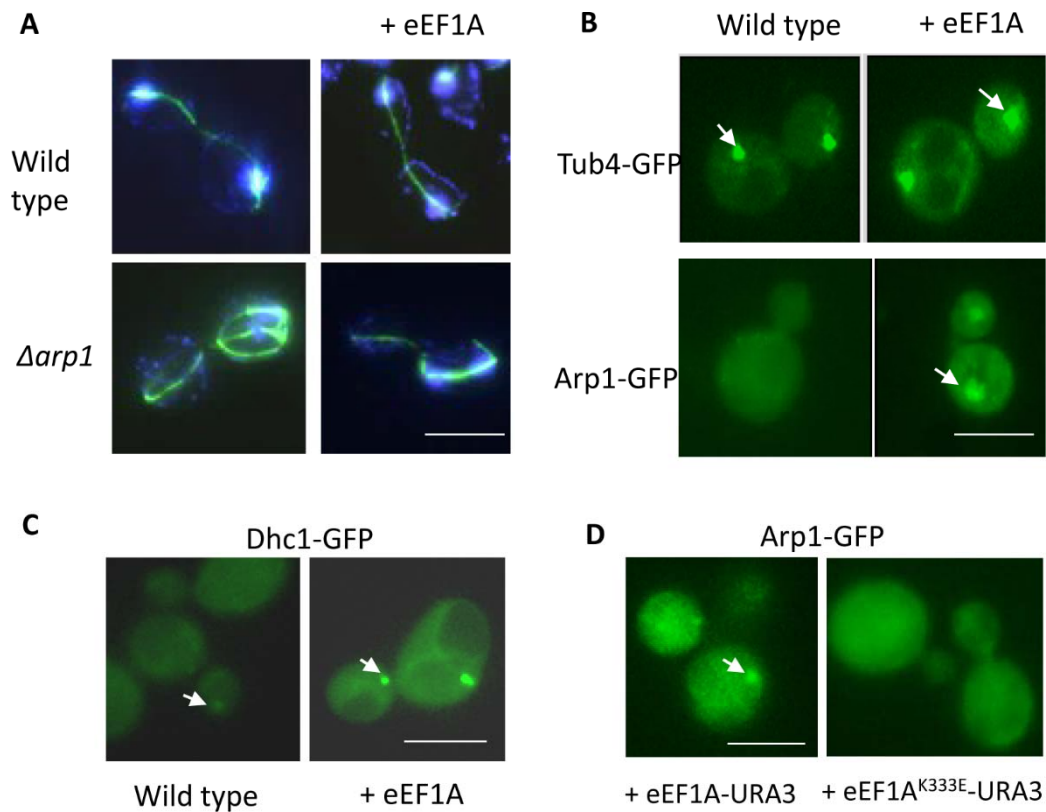software, n=100 (E). Error bars represent standard deviation, ***P<0.001, **P<0.01, *P<0.05.

Figure 3 – Immunofluoresence was used to visualise β-tubilin (green) and DNA (blue) in wild type and *Δarp1* cells containing an empty or eEF1A overexpression plasmid (A). The spindle pole body (TUB4-GFP, γ-tubulin) or ARP1-GFP (dynamin) were observed in dividing wild type cells containing an empty control or eEF1A overexpression plasmid (B). GFP labelled Dynein heavy chain (Dhc1) was observed in log phase cells containing an empty control or eEF1A overexpressing plasmid (C). A construct expressing eEF1A -URA3 or eEF1A^{K333A} was introduced into wild type cells and ARP1-GFP visualised using fluorescence microscopy (D). Arrows identify proteins localised to the spindle pole body in all cases, Size bar = 10μm.
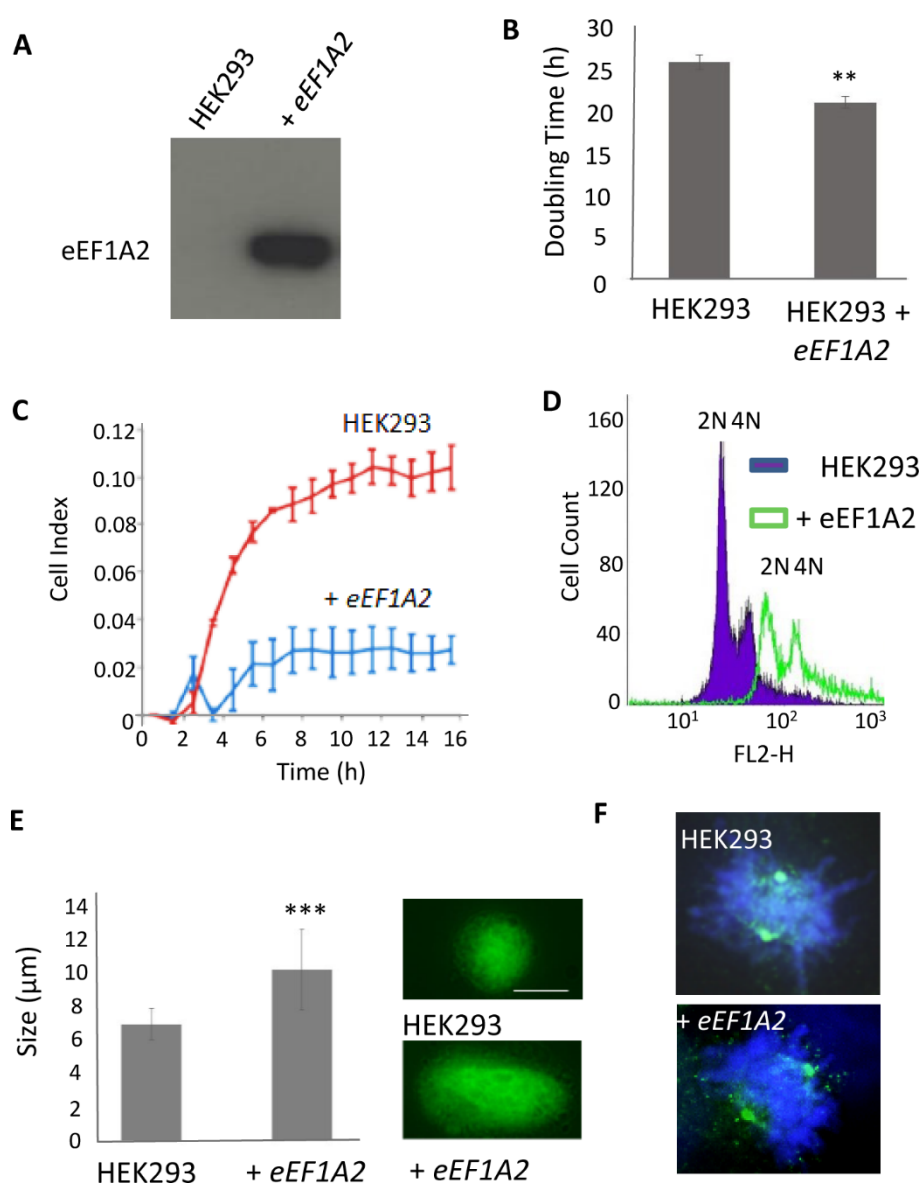
Figure 4 – A stable HEK293 eEF1A2 expression cell line was generated and confirmed by western blot (A). The effects of eEF1A2 expression upon growth rate of HEK293 cells was assessed in biological triplicate using and xCelligence analyser, n = 3 (B). The rate of attachment of HEK293 and HEK293 + eEF1A2 cells to the growth surface was assessed using an xCelligence analyser (C). DNA content of actively growing HEK293 and HEK293 + eEF1A2

cells was assessed in fixed cells by propidium iodide staining and FACS analysis (D) and visually by fluorescence microscopy (E), nuclear size was calculated using image J software (n=80, size bar=8µm). γ-tubulin (green) distribution within mitotic HEK293 and HEK293 + eEF1A2 cells were assessed by immunofluorescence, cells were co-stained with DAPI (blue) (F). Error bars represent standard deviation, ***P<0.001, **<0.01.
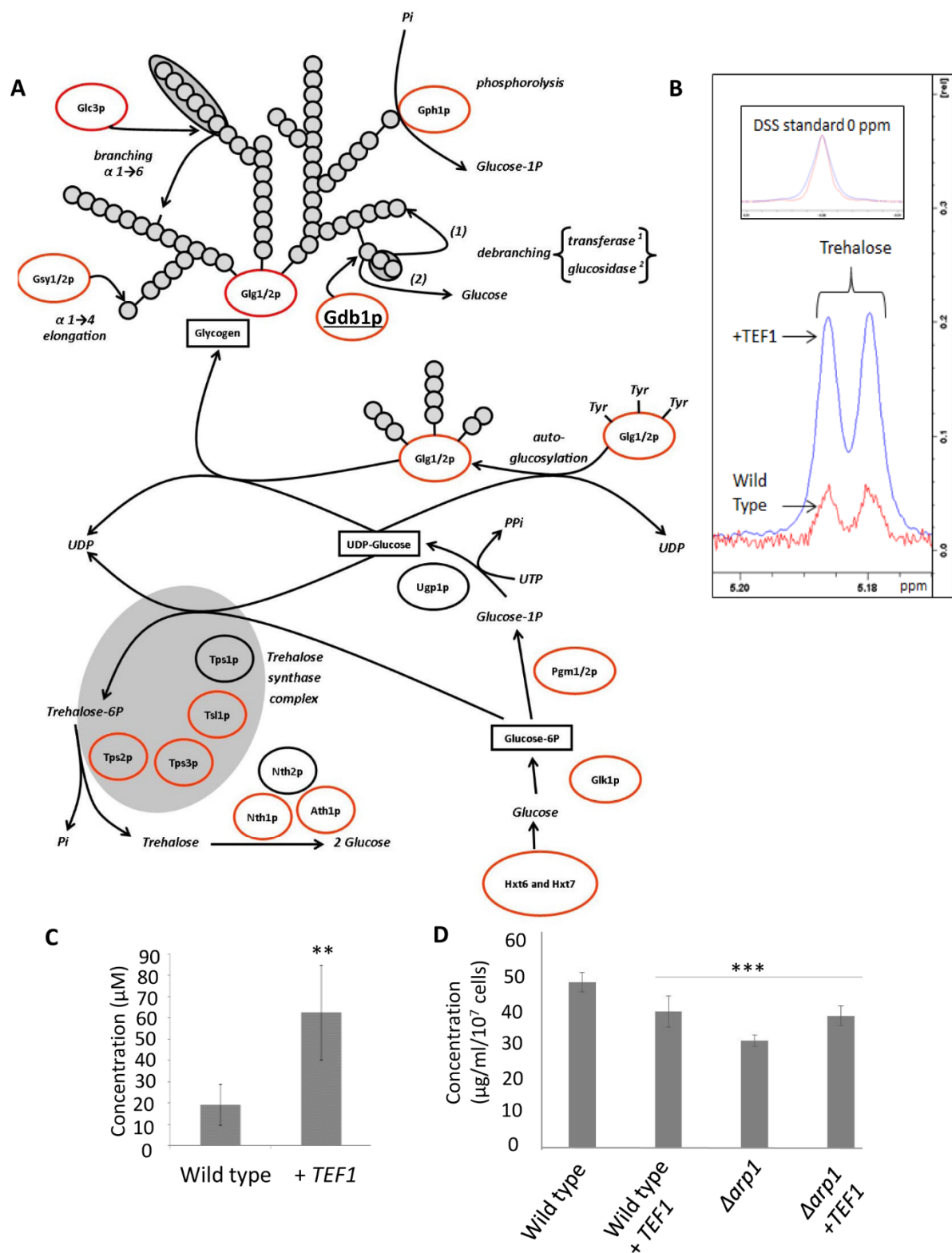
Figure 5 - A microarray analysis was carried out in yeast cells to determine the effects of

eEF1A overexpression on global gene expression during log phase of growth. The genes

identified as upregulated within the processes of glucose uptake and storage as trehalose or

glycogen upon overexpression of eEF1A are circled in red (A). The glycogen debranching

enzyme Gdb1, which possesses both α-1,4-glucanotransferase and α-1,6-glucosidase activity

(Teste et al., 2000), has been underlined to highlight its upregulation (A). The elevation of

trehalose during log phase was confirmed using quantative NMR, the peaks used for

assignment are presented (B), and levels quantified with reference to a known DSS standard

(C). The accumulation of glycogen in response to eEF1A overexpression was assessed in log

phase wild type and *Δarp1* cells using a biochemical assay as outlines in materials and

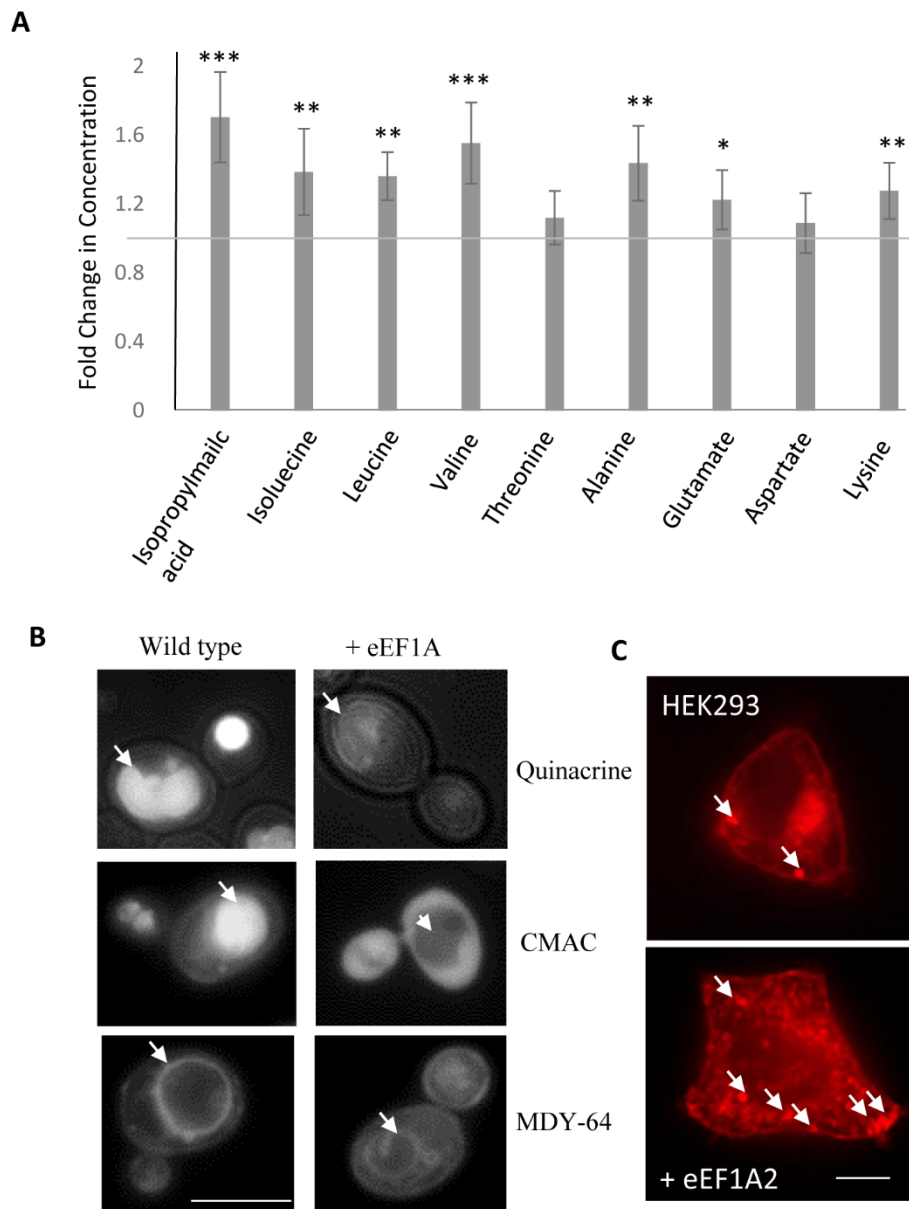methods (D). Error bars represent standard deviation, ***P<0.001, **P<0.01.

Figure 6 – NMR was used to quantify levels of a number of metabolites in extracts prepared from log phase wild type yeast cells containing a control or eEF1A overexpression plasmid, data is presented as fold change compared to wild type, n = 6 (A). Vacuole function was assessed in wild type control and eEF1A overexpressing cells using fluorescent dyes, Quinacrine, CMAC and MDY-64, arrowheads indicate the yeast vacuole (B). Lysosomes were stained in HEK293 control or eEF1A2 expressing cells using lysosensor dye and visualised by fluorescence microscopy, arrowheads indicate lysosomes (C). Size bar = 10μm. Error bars represent standard deviation, ***$p < 0.001$, **$p < 0.01$, *$p < 0.05$.

Table 1 – Metabolites were prepared from wild type control or eEF1A overexpressing cells by a boiling ethanol extraction procedure. Samples were then subjected to proton NMR and the concentrations of a number of identifiable metabolites were calculated as described within materials and methods. Averages of six biological replicates are presented and standard deviation is presented, ***P<0.001, **P<0.01, *P<0.05.

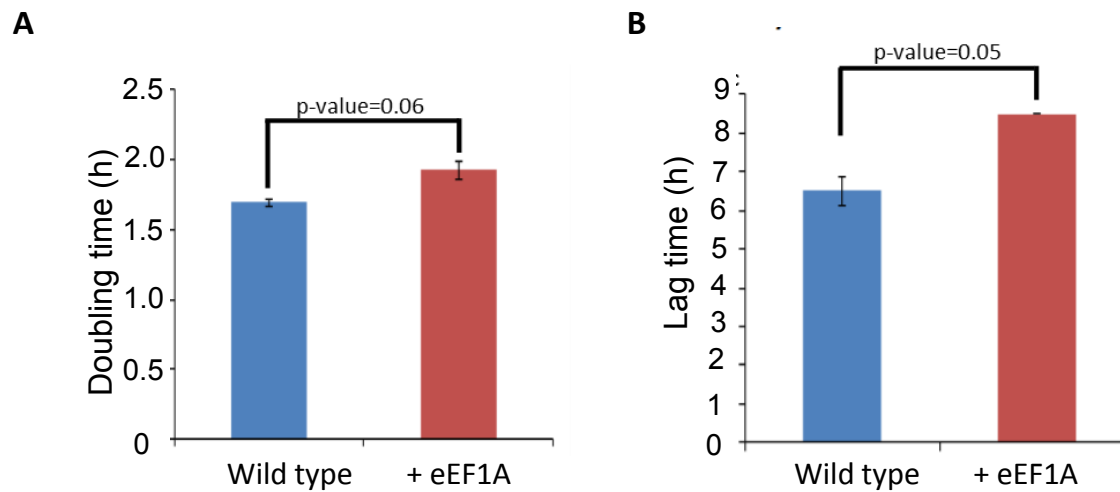| Metabolite	Wild Type + empty plasmid (µM)	Wild Type + *TEF1* (µM)
Isopropylmalic acid	111.6 ± 6.4	190.2 ± 29.4***
Isoleucine	74.2 ± 4.4	90.0 ± 11.9**
Leucine	37.0 ± 5.9	50.4 ± 5.2
Valine	80.5 ± 8.8	125 ± 18.9**
Threonine	453.3 ± 32.7	507.9 ± 70.6
Alanine	409.3 ± 41.6	587.9 ± 89.0*
Aspartate	246.9 ± 19.1	290.3 ± 33.1*
Acetic Acid	707.9 ± 123.1	679.6 ± 99.5*
NADH	115.3 ± 7.7	97.0 ± 10.6***
Trehalose	19 ± 9.6	75.2 ± 26.8***
Glutamtae	1.23 ± 0.11	1.5 ± 0.22**
Lysine	1.05 ± 0.07	1.35 ± 0.17

Figure S1 - An empty control plasmid or one containing eEF1A under the control of a GPD promoter was introduced into a wild type yeast strain and grown on selective media within an automatic plate reader and readings taken every 30 min. The doubling time (A) and time to initiation of growth (lag phase, B) were calculated from three independent biological experiments.
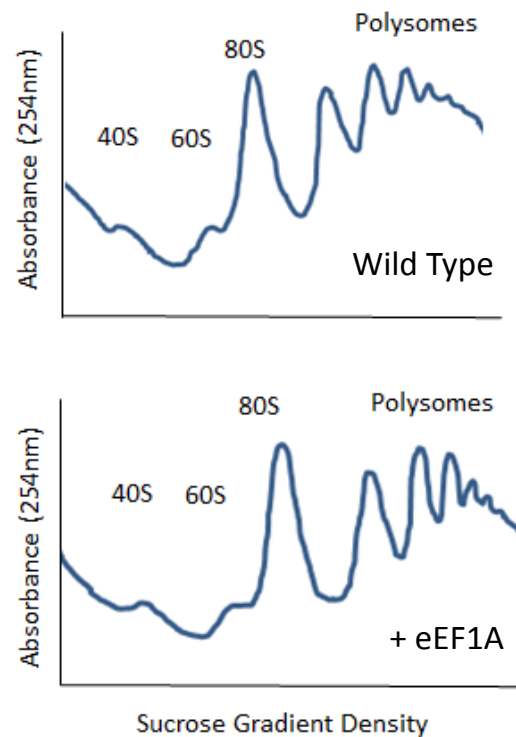
Figure S2 – Extracts were prepared from wild type cells carrying an empty control or eEF1A overexpression plasmid that had been grown to log phase in selective media. Cells were lysed and fractionated to isolate ribosomal fractions whose absorbance was measured at 254nm to obtain ribosomal profiles. The peaks representing small subunit (40S), large subunit (60S), intact ribosomes (80S) and polysomes are indicated.
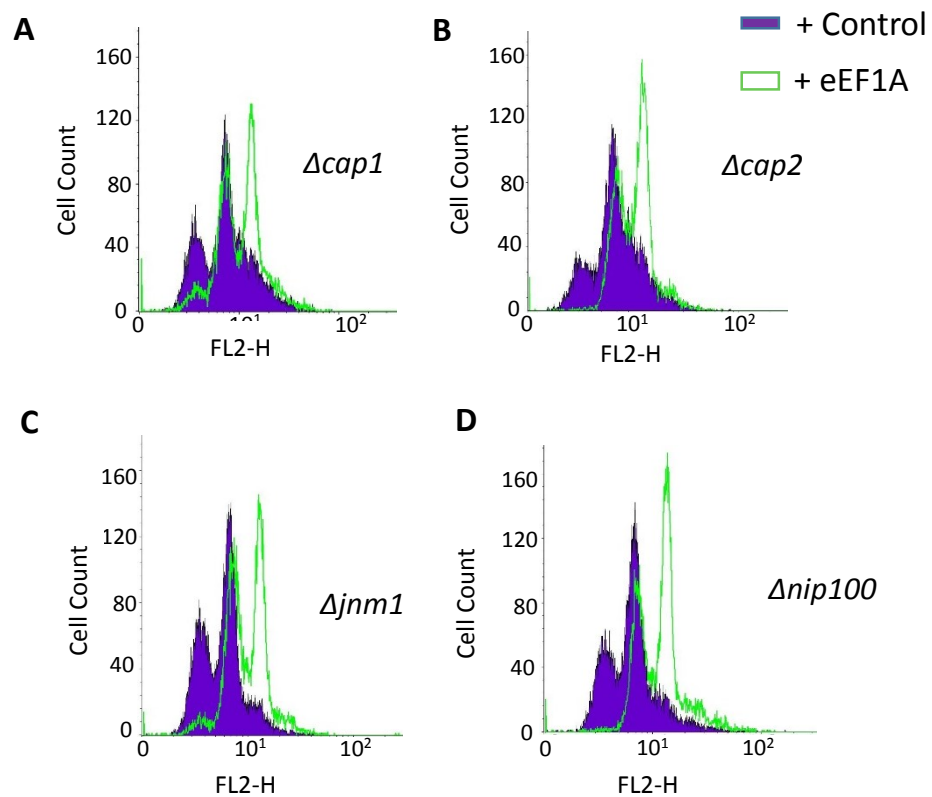
Figure S3 – DNA content was analysed in Wild type or *Δcap1, Δcap2, Δjnm1 and Δnip100* cells containing a control plasmid (filled) or eEF1A overexpression (open) plasmid by FACS analysis
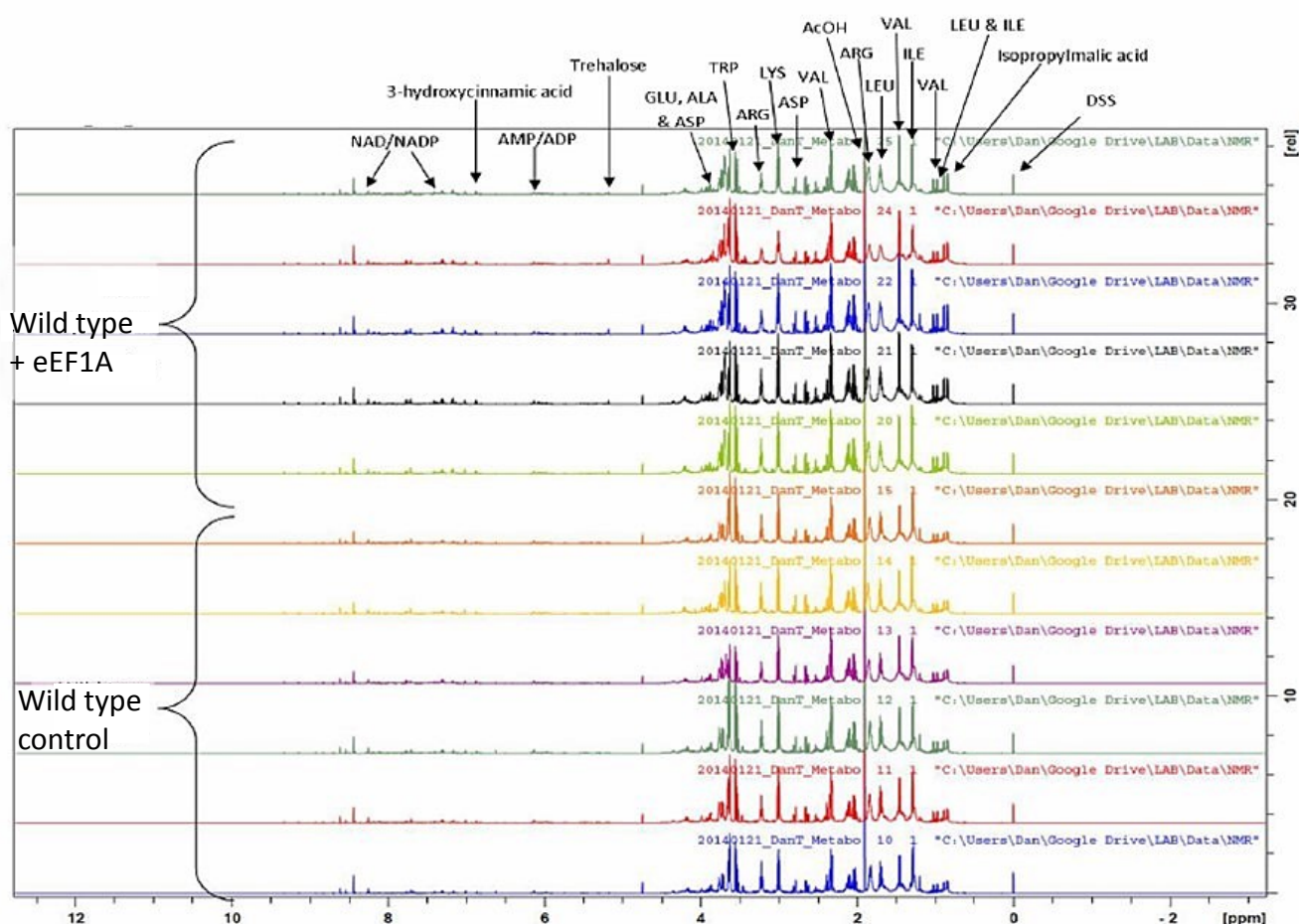
Figure S4 – Metabolites were prepared from wild type control or eEF1A overexpressing cells by a boiling ethanol extraction procedure. Samples were then subjected to proton NMR and are presented as a 1D spectra. Samples were prepared and analysed in six biological replicates. Metabolites that could be identified are indicated by arrows.

Table S1 – Yeast strains used in this study

Strain	Genotype	Source
BY4741 (Wild type)	*MATa his3•1 leu2•0 met15•0 ura3•0*	Source Bioscience
•arp1	*MATa his3•1 leu2•0 met15•0 ura3•0 arp1::KANMX*	Source Bioscience
•cap1	*MATa his3•1 leu2•0 met15•0 ura3•0 cap1::KANMX*	Source Bioscience
•cap2	*MATa his3•1 leu2•0 met15•0 ura3•0 cap2::KANMX*	Source Bioscience
•jnm1	*MATa his3•1 leu2•0 met15•0 ura3•0 jnm1::KANMX*	Source Bioscience
•nip100	*MATa his3•1 leu2•0 met15•0 ura3•0 nip100::KANMX*	Source Bioscience
ARP1-GFP	*MATa his3•1 leu2•0 met15•0 ura3•0 ARP1-GFP::HIS3*	Huh et al, 2003
TUB4-GFP	*MATa his3•1 leu2•0 met15•0 ura3•0 TUB4-GFP::HIS3*	Huh et al, 2003
DHC1-GFP	*MATa his3•1 leu2•0 met15•0 ura3•0 DHC1-GFP::HIS3*	Huh et al, 2003

Table S2 – Wild type control or eEF1A overexpressing cells were assessed for DNA content by FACS analysis (10.000 cells) and the percentage of cells within each peak calculated. The percentage of multinucleate cells was determined by fluorescence microscopy (n=200).

Strain	FACS Analysis				Microscopy
	Peak 1	Peak 2	Peak 3	Peak 4	% of multinucleate cells
Wild type	32.7	54.2	7.0		0.46
Wild type + *eEF1A*	29.6	59.9	6.0		0.43
Δarp1	22.0	53.9	15.1	5.0	20.83
Δarp1 + eEF1A	3.7	37.9	49.3	7.3	30.52

Table S3 – Wild type control or eEF1A overexpressing cells were assessed for changes in gene expression using microarray. The genes that were assessed as being upregulated upon eEF1A overexpression are presented following analysis for their involvement within a cellular process on the basis of gene ontology using the slim mapper tool.

GO Process	Gene(s) Up regulated
carbohydrate transport	GLK1,HXT7,HXT6,HXT1,HXT9,GAL2
oligosaccharide metabolic process	TPS1,NTH1,TPS2,HSP104,TSL1,SNF2
lipid transport	DRS2,SWH1,OSH2,DNF2,DNF1,SUT1,PRY3,UPS1,FAA1
cytokinesis	CDC15,BOI1,SDS24,BOI2,DSE2,SWE1,MYO3,CHS5,VRP1,MYO5,ZDS1,BNI1,THP1
response to osmotic stress	CYC8,GPD1,NRG1,GPP2,GRE3,SLN1,MYO3,SSK1,MYO5,TCO89,HSP82,OPY2
endocytosis	DRS2,SWH1,ECM21,SDS24,OSH2,DNF2,DNF1,MYO3,ENT2,VRP1,MYO5,SCD5
amino acid transport	BAP2,RTC2,AVT6,AUA1,MUP3
cellular amino acid metabolic process	ADH5,HIS7,ILV6,HIS4,CIT2,LYS14,HOM2,UME6,TRP4,HOM3,TRP2,UGA1,ARG4,THR1,CPA2,MAE1,OXP1,SRY1,DPS1,MET17,LEU3,ARG7,IDH1,MET4,IDH2,CDC60,ASN1
cell budding	BOI1,BOI2,KIC1,MYO3,VRP1,MYO5
carbohydrate metabolic process	UBP14,TPS1,ADH5,GLK1,CIT2,NTH1,TPS2,UME6,GLC3,GPP2,SAK1,IGD1,PYC1,SOL4,GRE3,TDH1,GLG1,HSP104,GAL2,GSY2,CHS5,YLR345W,TSL1,PFK2,GLO4,SNF2,TCO89
protein folding	CNE1,SSE2,AHA1,EUG1,HSP104,SSE1,FLC1,HSP82,CIN2
response to starvation	SUT1,SIP2,CLG1,PCL5,TAX4,ATG2,SNF2,OPY2,ATG13
protein maturation	MAP2,DAP2,RAM2,ATG19
generation of precursor metabolites and energy	ADH5,GLK1,GLC3,RGI1,IGD1,SHY1,TDH1,GLG1,GSY2,YLR345W,ISF1,PFK2,IDH1,IDH2
ion transport	DRS2,BAP2,RTC2,DNF2,PIC2,AVT6,DNF1,AUA1,FET5,TPO2,YHL008C,MUP3,YKE4,COX19,UPS1,PFK2,ATO2,COT1,FAA1,FLC1
response to heat	TPS1,TPS2,AHA1,HSF1,HSP104,SIN3
exocytosis	SWH1,OSH2,MYO3,MYO5
cell wall organization or biogenesis	ROT2,YPS7,KIC1,MHP1,TAX4,GON7,MYO3,YPS3,CHS5,MYO5,KRE1,HRD1,HPF1,TCO89,FLC1

GO Process	Gene(s) Up regulated
cell morphogenesis	DOT6,KIC1
biological process unknown	FUN19,BDH2,MOH1,YBL113W-A,PAR32,YDR545C-A,GTT3,YEL043W,YEL077W-A,YER053C-A,YER079W,YER134C,YER152C,YER190C-B,YFL042C,YFL067W,YFL068W,YFR018C,YFR035C,YGL117W,YGR127W,YGR237C,YGR296C-B,AIM17,YHL050W-A,YHR219C-A,YIL060W,YIL092W,ASG1,OM45,YIL177W-A,REE1,YJL225W-A,YKL023W,SEG2,PMU1,YLL066W-A,YLL067W-A,SKG3,YLR278C,YLR326W,YLR466C-A,YLR467C-A,NAB6,YML133W-B,YMR105W-A,YMR160W,ICY1,YMR196W,YNL034W,TOS6,YNL339W-B,YNR014W,YNR034W-A,YOL029C,YOL131W,YOL159C,YOR012W,YOR396C-A,YPL109C,YPL283W-B,YPR204C-A

Table S4 – Wild type control or eEF1A overexpressing cells were assessed for changes in gene expression using microarray. The genes that were assessed as being downregulated upon eEF1A overexpression are presented following analysis for their involvement within a cellular process on the basis of gene ontology using the slim mapper tool.

GO Process	Gene(s) Down regulated
mitochondrial translation	PET122,RRF1,PTH1,MRPL38, MRPL33
transcription from RNA polymerase I promoter	RRN3,RPB10
carbohydrate transport	HXT17
pseudohyphal growth	PGU1,HMS1
transcription from RNA polymerase III promoter	RPB10
snoRNA processing	RRP45
ribosomal small subunit biogenesis	LOC1,FCF2,FYV7
rRNA processing	RRP45,NUG1,LOC1,FCF2,FYV 7,RMP1,PUS7
protein folding	EMC5,CUR1
ribosomal large subunit biogenesis	NOP16,LOC1
ribosomal subunit export from nucleus	NUG1
tRNA processing	FMT1,PUS7
mitochondrion organization	PET122,RRF1,PTH1,MRPL38, COX17,MRPL33
translational initiation	DED1
lipid transport	RFT1
DNA-dependent transcription, initiation	RRN3
sporulation	SPO73,RIM9
biological process unknown	YAR023C,YBR298C-A,YCR024C-B,YCR100C,BSC1,NKP1,YGR1 74W-A,MTC6,RRT14,YLR363W-A,YLR412C-A,AIM34,YMR030W-A,YMR230W-A,KSH1,YNL162W-A,YPR153W